journal

J. Am. Ceram. Soc., **88** [12] 3423–3426 (2005)
DOI: 10.1111/j.1551-2916.2005.00614.x

Fabrication and Efficient Infrared-to-Visible Upconversion in Transparent Glass Ceramics of Er–Yb Co-Doped CaF_2 Nano-Crystals

Yuki Kishi and Setsuhisa Tanabe*,†

Graduate School of Human and Environmental Studies, Kyoto University, Sakyo-ku, Kyoto 606-8501, Japan

Shigemi Tochino and Giuseppe Pezzotti

Department of Chemistry and Materials Technology, Ceramic Physics Laboratory & Research Institute for
Nanoscience, RIN, Kyoto Institute of Technology, Matsugasaki, Sakyo-ku, Kyoto 606-8585, Japan

Transparent glass ceramics containing CaF_2 nano-crystals co-doped with Er–Yb were developed by heat treatment of glasses in the system SiO_2–Al_2O_3–CaF_2–LnF_3 (Ln = Er, Yb). The crystal size of CaF_2 increased with increasing heat-treatment temperature. Upconversion emission intensities at 660 and 540 nm increased dramatically with increasing heat-treatment temperature. The cathode luminescence mapping indicates that the visible Er-luminescence arises mainly from the precipitated CaF_2 nano-crystals with a phonon energy lower than that of a silicate matrix. It is concluded that both Er and Yb were concentrated in the CaF_2 nano-crystals, and the quantum efficiency of Er^{3+}-luminescence and the energy transfer efficiency from Yb^{3+} were considerably improved after ceramization.

I. Introduction

In recent years, the near infrared (NIR) to visible (VIS) and ultraviolet (UV) upconversion luminescence by rare-earth ions-doped materials has been investigated, due to the possibility of all-solid-state upconversion lasers operating in the VIS and UV spectral range. Also, the potential applications in areas such as color display, optical data storage, and sensor can be expected. Optical properties of trivalent lanthanide ions such as Er^{3+}, Tm^{3+}, and Ho^{3+} in glasses, crystals, or glass ceramics have been extensively studied to develop visible upconversion lasers and optical amplifiers for telecommunication.[1–4] Among the trivalent lanthanide ions, the upconversion process of Er^{3+} ion has been widely investigated in various kinds of host materials.[5,6] The sensitization of Er^{3+} emission with Yb^{3+} ions is a well-known phenomenon for increasing the optical pumping efficiency for 1.5 and 0.55 μm applications because of the efficient energy transfer from Yb^{3+} to Er^{3+} ions.[7] Host materials with a low phonon energy for Er^{3+} ions can reduce the multi-phonon relaxation, and thus a high-efficiency upconversion luminescence can be obtained. Fluoride glass and crystal, which have a phonon energy lower than that of oxide glass, are well known as good host material for lanthanide ions.[8] However, for practical applications, oxide glasses have an advantage superior to fluoride due to their chemical durability, thermal stability, and mechanical strength. Oxy-fluoride glass ceramics with the advantage of both fluoride and oxide materials have been studied since 1993.[9–12] In these studies, highly efficient upconversion luminescence of lanthanide ions in PbF_2 and CdF_2 nano-crystals, precipitated in a silicate glass matrix, was obtained. Today, the demand for alternative materials of Pb and Cd is growing, since they have been designated as specified toxic substances by the restriction hazardous substance (RoHS). The CaF_2 has the same fluorite structure as the β-PbF_2, and also has good transparency in the near UV to middle IR range. Therefore, CaF_2 can be expected for use as a good alternative material for PbF_2. In 2002, Fu *et al.*[13] reported on the optical properties of divalent Eu^{2+} ions in glass ceramics containing CaF_2 crystal. In this study, oxy-fluoride glass ceramics containing CaF_2 nano-crystals co-doped with trivalent Yb^{3+} and Er^{3+} ions were fabricated, and the upconversion luminescence properties were investigated.

II. Experimental Procedure

Oxy-fluoride glasses in the system $45SiO_2$–$20Al_2O_3$–$10CaO$–$xCaF_2$–$yYbF_3$–$zErF_3$ $z = 1, 0.5$), where (x, y) is (20, 5) or (22, 2), were prepared by the melting method; 20 g batches in a platinum crucible were melted at 1300°C for 1 h. The glass transition temperature (T_g) and the onset of crystallization temperature (T_x) were measured by differential thermal analysis (DTA) measurement (Rigaku, Tokyo, Japan, Thermal plus, TG-DTA TG8120). Glass ceramics containing CaF_2 were prepared by heat treatment at 700°–780°C for 4 h. The crystal phases precipitated in the glass matrix were identified by X-ray diffraction (XRD) measurement (Shimadzu, Kyoto, Japan, XRD6000). The scanning electron microscopy (SEM) image at the fracture surface of the glass ceramic sample was measured by field emission (FE)-SEM (JEOL, Tokyo, Japan, JSM-6500M). The upconversion spectra in the visible range of Er^{3+} in oxy-fluoride glass and glass ceramics were measured by pumping with a 970 nm laser diode (LD) (SDL, 6362-P1), and using a monochromator (Nikon, Tokyo, Japan, G-250) and a photo-multiplier (Hamamatsu Photonics, Hamamatsu, Japan, E717–37). Cathode luminescence spectra from the area of SEM observation of the glass ceramic sample heat treated at 780°C were measured by a cathode luminescence spectroscopic system (JOBIN YVON, St.-Genis-Pouilly, France, CLM-32, TRIAX320).

III. Results

(1) Oxy-Fluoride Glass Ceramics Containing CaF_2 Nano-Crystals

Figure 1 shows the DTA curve of the as-made glass of $(x, y, z) = (20,5,1)$ composition. The glass transition temperature, T_g, the onset of CaF_2 crystallization temperature, T_x, and the crystallization temperature of oxide matrix, T_c, were estimated to be 620°, 702°, and 872°C, respectively. Figure 2 shows XRD patterns of Er–Yb co-doped glass and glass ceramics heat treated at 700°–750°C. It can be seen that the single phases of CaF_2 crystals were precipitated in the glass matrix by heat treatment. Figure 3 shows the SEM images at the fracture surface of glass

---

J. Ballato—contributing editor

Manuscript No. 20246. Received March 2, 2005; approved May 22, 2005.
Supported by the Grants-in-Aid for Scientific Research (No.16360329) from the Ministry of Education, Science and Culture, Japan.

*Member, American Ceramic Society (107396).

†Author to whom correspondence should be addressed. e-mail: stanabe@gls.mbox.media.kyoto-u.ac.jp

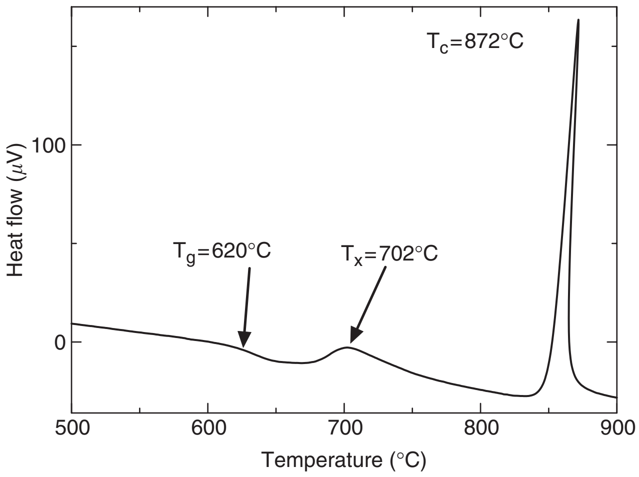

Fig. 1. Differential thermal analysis curve of $45SiO_2$–$20Al_2O_3$–10CaO–$22CaF_2$–$2YbF_3$–$1ErF_3$ glass.

ceramics heat treated at 700° and 750°C. The average crystal size of CaF_2 was about 20 nm with heat-treatment at 700°C and increased up to 40 nm with heat treatment at 750°C.

(2) Upconversion of Er^{3+} in Glass Ceramics

Figure 4 shows upconversion spectra of Er^{3+}–Yb^{3+} co-doped glass and glass ceramics of all compositions. No upconversion luminescence was observed in the as-made glasses, while green-upconversion at 540 nm due to the $^4S_{3/2} \rightarrow {}^4I_{15/2}$ transition and red-upconversion at 660 nm due to the $^4F_{9/2} \rightarrow {}^4I_{15/2}$ were observed in all the glass ceramics.

(3) Cathode Luminescence Measurement

Figure 5 shows the cathode luminescence spectra collected at a glass matrix point and at a fluoride crystal phase point as indicated by the number in Fig. 6. Emissions at 540 and 660 nm were observed in both the glass matrix and crystal phase. Figure 6 shows the mapping image of cathode luminescence monitored at 660 nm of the $45SiO_2$–$20Al_2O_3$–10CaO–$22CaF_2$–$2YbF_3$–$1ErF_3$ glass ceramics heat treated at 780°C. In the mapping image, dots of the crystal phase area (100 nm) with strong red-upconversion appears bright in color.

IV. Discussion

(1) Oxy-Fluoride Transparent Glass Ceramics Containing CaF_2 Nano-Crystals

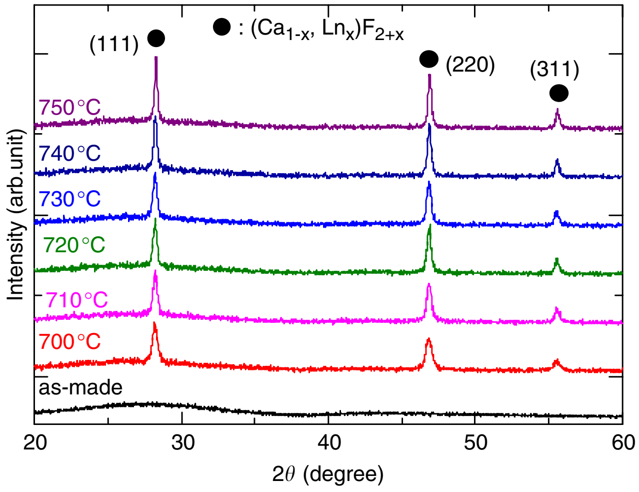

Fig. 2. X-ray diffraction pattern of Er^{3+}–Yb^{3+} co-doped glass and glass ceramics heat treated at 700°–750°C.

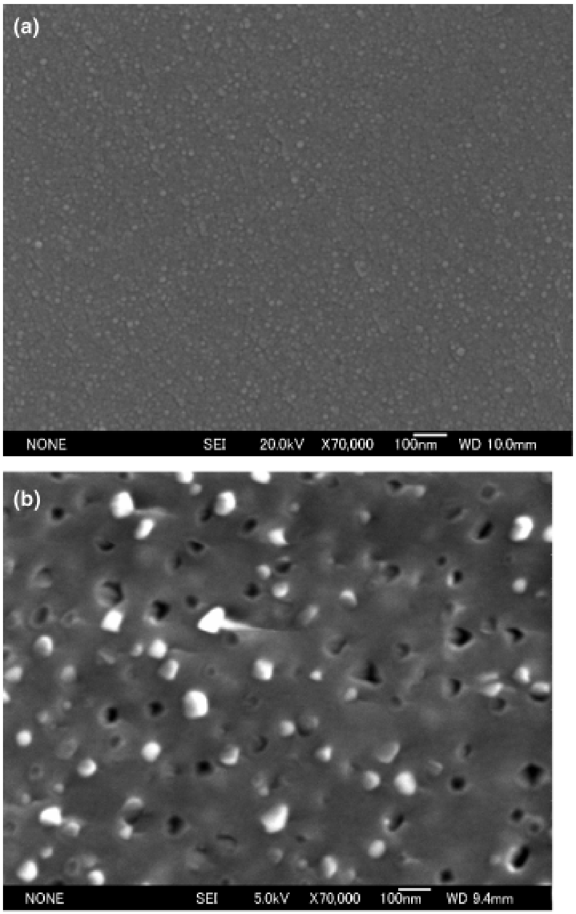

Fig. 3. Scanning electron microscopy image (× 70 000) at fracture surface of glass ceramics heat treated at (a) 700°C and (b) 750°C.

From the obtained peak width of XRD patterns shown in Fig. 2, the lattice constant, *a*, and crystallite size, *D*, of the CaF_2 crystal were estimated by using the Bragg's law and the following Sherrer's equation:

$$D = \frac{K\lambda}{\beta \cos\theta} \tag{1}$$

where β is the diffraction line-width, which was calculated after subtracting contributions of the strain in the crystallites by Hall's plot and the instrument constant from the measured value. Figure 7 shows the heat-treatment temperature dependence of the lattice constant and crystallite size of CaF_2 crystal. The crystallite size increased monotonically from about 20 to 40nm with increasing temperature. These values correspond to the observed size in the SEM images in Fig. 3. Figure 8 shows the phase diagram of the CaF_2–YbF_3 system.[14] CaF_2 and YbF_3 yield a solid solution in the range of about 0–35 mol% YbF_3 content. The lattice constant of the nano-crystals in the present glass ceramics was about 5.49 Å at any heat-treated temperature, larger than that of the pure CaF_2 crystal ($a = 5.46$Å). Therefore, the Yb^{3+} and Er^{3+} are considered to be incorporated into the CaF_2 to form $(Ca_{1-x}, Ln_x)F_{2+x}$ solid-solution crystals containing trivalent lanthanide ions, Yb^{3+} and Er^{3+}.

The present glass ceramics heat treated at 700°–750°C maintained good transparency. The main reason for transparency of these glass ceramics could be much smaller crystallite size (20∼40 nm) than the wavelength of visible light. It is concluded that the transparent glass ceramics containing $(Ca_{1-x}, Ln_x)F_{2+x}$ nano-crystals were fabricated in these compositions.

(2) Upconversion of Er^{3+} in Glass Ceramics

Figure 9 shows a possible upconversion mechanism of Er^{3+}–Yb^{3+} with 970 nm pumping. By the energy transfer from Yb^{3+}

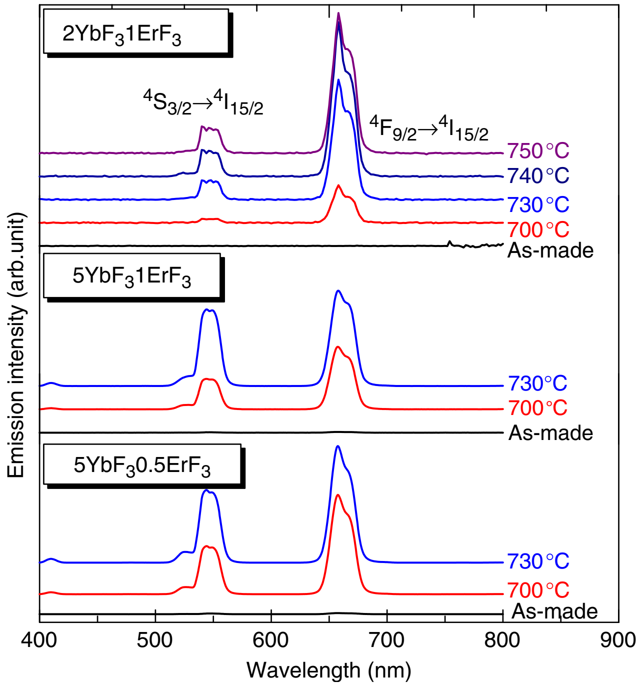

Fig. 4. Upconversion spectra of (a) $22CaF_2$–$2YbF_3$–$1ErF_3$, (b) 20CaF2–$5YbF_3$–$1ErF_3$, (c) $20CaF_2$–$5YbF_3$–$0.5ErF_3$-doped glass and glass ceramics heat treated at 700°–750°C.

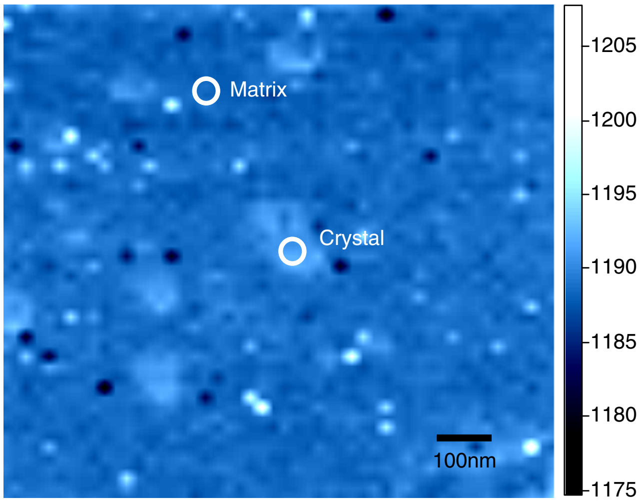

Fig. 6. Mapping image of red-upconversion at 660 nm of $45SiO_2$–$20Al_2O_3$–10CaO–$22CaF_2$–$2YbF_3$–$1ErF_3$ glass ceramics heat treated at 780°C by cathode luminescence (CL).

ions pumped by 970 nm LD, Er^{3+} ions are excited to the $^4F_{7/2}$ level by two-step process and are relaxed to lower energy levels such as the $^4S_{3/2}$ and $^4F_{9/2}$ by multi-phonon relaxation. As shown in Fig. 4, no upconversion luminescence was observed in the as-made glasses, while upconversion emissions at 540 and at 660 nm (Er^{3+}) were observed in glass ceramics. Figure 10 shows the heat-treatment temperature dependence of the integrated intensity of 540 and 660 nm emission bands in $45SiO_2$–$20Al_2O_3$–10CaO–$22CaF_2$–$2YbF_3$–$1ErF_3$ glass ceramics. Both intensities increased dramatically with increasing heat-treatment temperature. After crystallization, the Yb^{3+} and Er^{3+} ions were incorporated into CaF_2 crystals with a lower phonon energy ($\hbar\omega = 400$ cm^{-1}) than SiO_2 ($\hbar\omega = 1100$ cm^{-1}) by heat treatment. Since the lifetimes of most excited levels of Er^{3+} ions are largely affected by the multiphonon decay rate, which is exponentially dependent on the inverse phonon energy of host materials, the multi-step excitation efficiency and radiative quantum efficiency for visible upconversion luminescences can be dramatically improved when Er^{3+} ions are incorporated into a low-phonon-energy environment. Also, upconversion luminescence efficiency of glass ceramics can be improved by promoting the two-step excitation due to the energy transfer from Yb^{3+} to Er^{3+} ions by decreasing the distance between Yb^{3+} and Er^{3+} ions in the CaF_2 crystal phases.

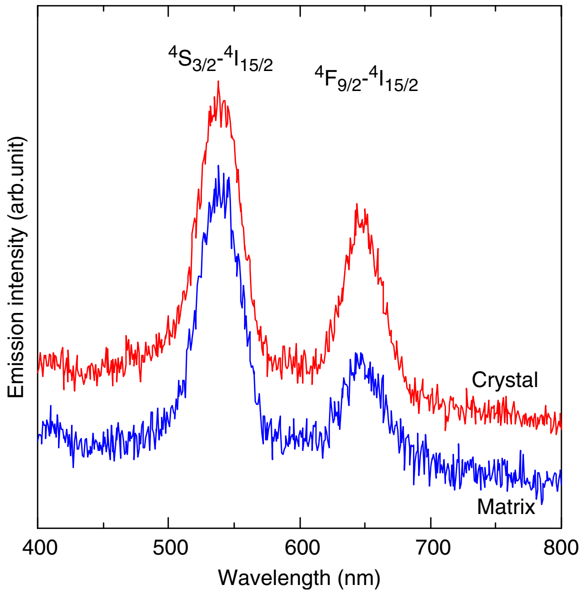

Fig. 5. Cathode luminescence spectra of the glass matrix point and the fluoride crystal phase point in the $45SiO_2$–$20Al_2O_3$–10CaO–$22CaF_2$–$2YbF_3$–$1ErF_3$ glass ceramics.

Green-upconversion intensity of the sample containing $5YbF_3$ was larger than that of the sample containing $2YbF_3$. It is indicated that the green-upconversion intensity of Er^{3+} also depends on the concentration of Yb^{3+}.[15] For the samples with a low [Yb]/[Er] ratio, the relative intensity of 660 nm/540 nm is high. The following energy transfer in adjacent Er^{3+} ions can occur easily, since the average distance between Er^{3+} ions is smaller:

$$({}^4S_{3/2} \rightarrow {}^4F_{9/2} : \mathrm{Er}^{3+}) \Rightarrow ({}^4I_{9/2} \rightarrow {}^4F_{9/2} : \mathrm{Er}^{3+}) \qquad (2)$$

This energy transfer, as indicated in Fig. 9, populates the $^4F_{9/2}$, which is the initial level of 660 nm-emission. This is also indicated in the CL spectra in Fig. 5. The red emission intensity at

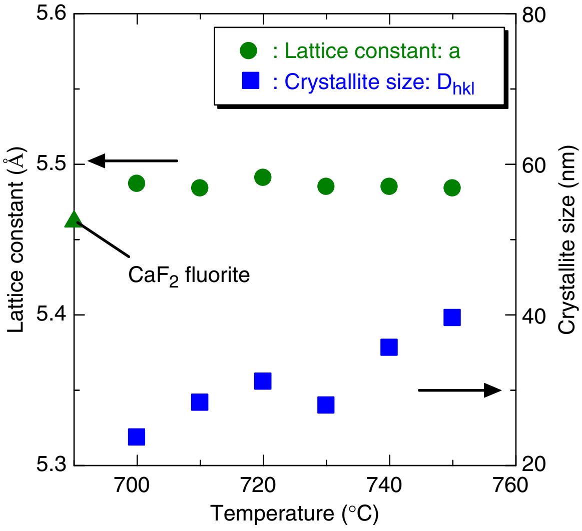

Fig. 7. Heat-treatment temperature dependence of the lattice constant and crystallite size of CaF_2 crystal in the glass ceramics.

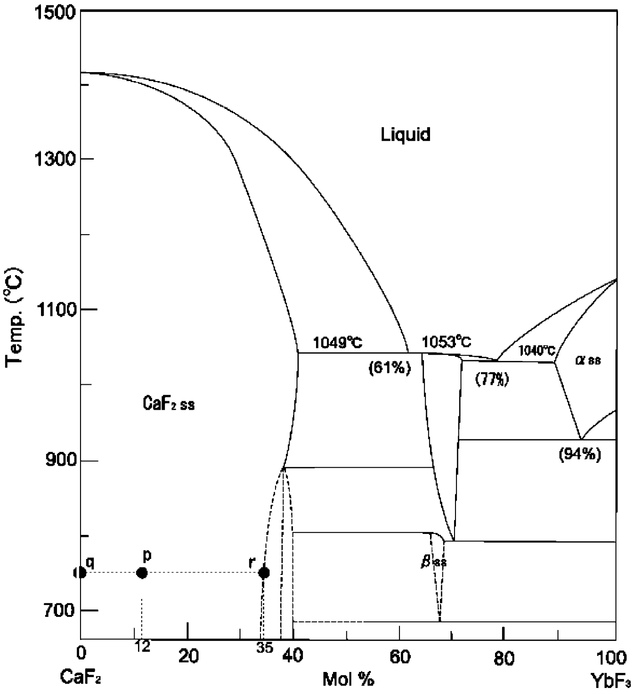

Fig. 8. Phase diagram of the CaF_2–YbF_3 system.[14]

660 nm of crystal phases was clearly larger than that of the glass matrix. As a result, the luminescence can be mainly observed from $(Ca_{1-x}, Ln_x)F_{2+x}$ nano-crystals as shown in Fig. 6. This is caused by the concentration of Er^{3+} and Yb^{3+} ions in crystal phases.

V. Conclusion

Er^{3+}–Yb^{3+}-doped transparent oxy-fluoride glass ceramic materials containing CaF_2 were prepared. Nano-crystals of $(Ca_{1-x}, Ln_x)F_{2+x}$ solid solution (Ln = Yb, Er) precipitated with size of 20–40 nm after heat-treatment at 700°–750°C. Green-upconversion luminescence at 540 nm and red-upconversion at 660 nm were observed in glass ceramics at 970 nm pumping. These results can be explained by considering that Yb^{3+} and Er^{3+} ions were incorporated into CaF_2 crystals with a phonon energy lower than that of silicate glass matrix.

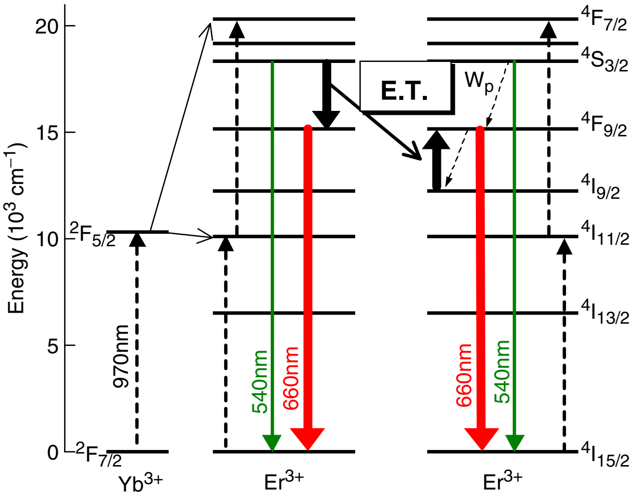

Fig. 9. Energy-level diagram of Yb^{3+} and Er^{3+} ions and a possible upconversion mechanism.

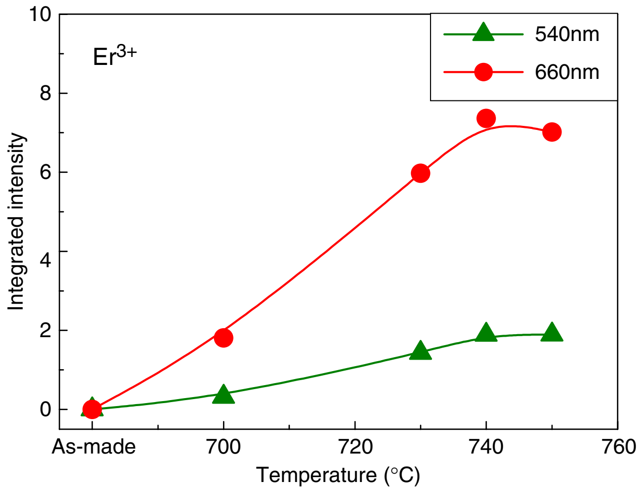

Fig. 10. Heat-treatment temperature dependence of the integrated intensity of 540 nm and 660 nm emission band in $45SiO_2$–$20Al_2O_3$–$10CaO$–$22CaF_2$–$2YbF_3$–$1ErF_3$ glass ceramics.

References

[1] J. S. Wang, E. M. Vogel, and E. Snitzer, “Tellurite Glass: A New Candidate for Fiber Devices,” *Opt. Mater.*, **3**, 187–203 (1994).

[2] S. Tanabe, “Optical Properties of Tm-Doped Tellurite Glasses for 1.4 μm Amplifier”; pp. 85–92 in Proceedings SPIE, Vol. 4282, *Rare-Earth-Doped Materials and Devices V* (Photonics West, Optoelectronics 2001, San Jose, January). Edited by S. Jiang, SPIE, Bellingham, WA, 2001.

[3] S. Tanabe, “Optical Properties of Tm and Er Ions in Novel Oxide Glasses for Amplifiers in Wavelength-Division-Multiplexing,” *Mater. Integration*, **13** [9] 39–45 (2000).

[4] S. Tanabe, H. Hayashi, T. Hanada, and N. Onodera, “Fluorescence Properties of Er^{3+} Ions in Glass Ceramics Containing LaF_3 Nanocrystals,” *Opt. Mater.*, **19**, 343–9 (2002).

[5] S. Tanabe, K. Suzuki, N. Soga, and T. Hanada, “Mechanisms and Concentration Dependence of Tm^{3+} Blue and Er^{3+} Green Upconversion in Codoped Glasses by Red-Laser Pumping,” *J. Lumines.*, **65** [5] 247–55 (1995).

[6] M. Takahashi, R. Kanno, Y. Kawamoto, S. Tanabe, and K. Hirao, “Compositional Dependence of Er^{3+} Upconversion Luminescence in MF–LiF–ZrF_4 Glasses (M: Alkali Metals),” *J. Non-Cryst. Solids*, **168** [1–2] 137–43 (1994).

[7] F. Auzel, “Upconversion Processes in Coupled Ion Systems,” *J. Lumines.*, **45**, 341–5 (1990).

[8] S. Tanabe and K. Hirao, “Blue Upconversion Laser Glass,” *Trans. IEE Jpn.*, **114-A** [6] 425–31 (1994).

[9] Y. Wang and J. Ohwaki, “New Transparent Vitroceramics Codoped with Er^{3+} and Yb^{3+} for Efficient Frequency Upconversion,” *Appl. Phys. Lett.*, **63**, 3268–70 (1993).

[10] P. A. Tick, N. F. Borrelli, L. K. Cornelius, and M. A. Newhouse, “Transparent Glass Ceramics for 1300 nm Amplifier Applications,” *J. Appl. Phys.*, **78**, 6367–70 (1995).

[11] M. J. Dejneka, “The Luminescence and Structure of Novel Transparent Oxyfluoride Glass–Ceramics,” *J. Non-Cryst. Solids*, **239**, 149–56 (1998).

[12] H. Hayashi, S. Tanabe, and T. Hanada, “1.4 μm Band Emission Properties of Tm^{3+} Ions in Transparent Glass Ceramics Containing PbF_2 Nanocrystals for S-Band Amplifier,” *J. Appl. Phys.*, **89** [2] 1041–5 (2001).

[13] J. Fu, J. M. Parker, P. S. Flower, and R. M. Brown, “Eu^{2+} Ions and CaF_2-Containing Transparent Glass–Ceramics,” *Mater. Res. Bull.*, **37**, 1843–9 (2002).

[14] B. P. Sobolev and X. Fedorov, “Phase Diagrams Of the CaF_2-(Y, Ln)F_3 Systems I. Experimental,” *J. Less-Common Met.*, **60** [1] 33–46 (1978).

[15] J. L. Sommerdijk, “On the Excitation Mechanisms of the Infrared-Excited Visible Luminescence in Yb^{3+}, Er^{3+}-Doped Fluorides,” *J. Luminesc.*, **4**, 441–9 (1971). □